Environmental Science & Technology

pubs.acs.org/est

Article

Multiple Effects of Humic Components on Microbially Mediated Iron Redox Processes and Production of Hydroxyl Radicals

Ruixia Han, Zhe Wang, Jitao Lv, Zhe Zhu, Guang-Hui Yu, Gang Li,* and Yong-Guan Zhu

Cite This: https://doi.org/10.1021/acs.est.2c03799

Read Online

ACCESS | Metrics & More | Article Recommendations | Supporting Information

ABSTRACT: Microbially mediated iron redox processes are of great significance in the biogeochemical cycles of elements, which are often coupled with soil organic matter (SOM) in the environment. Although the influences of SOM fractions on individual reduction or oxidation processes have been studied extensively, a comprehensive understanding is still lacking. Here, using ferrihydrite, *Shewanella oneidensis* MR-1, and operationally defined SOM components including fulvic acid (FA), humic acid (HA), and humin (HM) extracted from black soil and peat, we explored the SOM-mediated microbial iron reduction and hydroxyl radical ($^{\bullet}OH$) production processes. The results showed that the addition of SOM inhibited the transformation of ferrihydrite to highly crystalline iron oxides. Although FA and HA increased Fe(II) production over four times on average due to complexation and their high electron exchange capacities, HA inhibited 30−43% of the $^{\bullet}OH$ yield, while FA had no significant influence on it. Superoxide ($O_2^{\bullet-}$) was the predominant intermediate in $^{\bullet}OH$ production in the FA-containing system, while one- and two-electron transfer processes were concurrent in HA- and HM-containing systems. These findings provide deep insights into the multiple mechanisms of SOM in regulating microbially mediated iron redox processes and $^{\bullet}OH$ production.

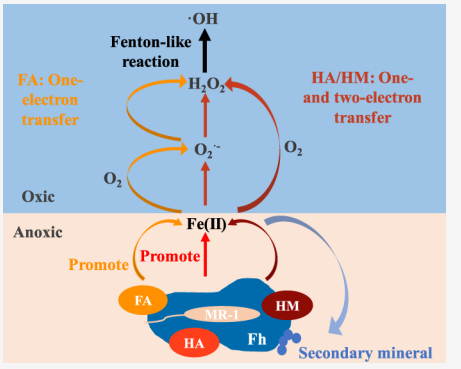

KEYWORDS: *soil organic matter, hydroxyl radical, iron, reactive oxygen species, redox cycle, dissimilatory iron-reducing bacteria*

INTRODUCTION

Microbial ferric iron (Fe(III)) reduction and reoxidation are widespread environmental processes under fluctuating redox conditions in soil that impact the biogeochemical cycling of elements including carbon, nitrogen, and trace metals.[1−3] Biochemical mechanisms of the electron transfer between iron-reducing bacteria and iron minerals have been widely investigated.[4−6] In the last two decades, the effects of mineralogical properties of iron oxy(hydr)oxides on microbial Fe(III) reduction and reactive oxygen species (ROS) production have also been revealed.[7−11] In soils and sediments, organic matter is closely associated with minerals and microbes, which makes their interactions more complex and unpredictable.[12]

Humic substances (HS) are major components of soil organic matter (SOM), which are operationally divided into fulvic acid (FA), humic acid (HA), and humin (HM). There are significant differences in chemical characterization and molecular structures for these three components. For example, FA contains molecules with lower molecular weight and higher oxygen content, while HA contains more polyaromatic hydrocarbons and heterocyclic hydrocarbons.[13−15] Particularly, HS contain many redox-active moieties, leading to different electron-donating and -accepting capacities (EDC/EAC) for HS components, which can serve as regenerable electron donors and acceptors in microbial respiration and further transfer electrons to other oxidants as redox buffers.[16,17] As well known, HS from different sources display distinct EAC and EDC.[18,19] Quinone/hydroquinone as well as non-quinone functional groups including thiols, disulfides, and phenazines in HS were found to be potential redox-active moieties, different contents of which caused various EDC and EAC for FA, HA, and HM.[18−23] It has been reported that HS promoted microbial iron reduction;[24−26] however, the influences of different components of HS on iron reduction efficiency and the formation of secondary minerals have not been comprehensively investigated.

According to previous studies, oxidation of ferrous iron (Fe(II)) and reduced HS can both produce ROS.[10,11,27−31] In an HS-free system, the production of hydroxyl radicals ($^{\bullet}OH$) upon oxidation of Fe(II) involved the formation of superoxide ($O_2^{\bullet-}$) and hydrogen peroxide (H_2O_2), followed one- and/or two-electron transfer pathways in different iron-containing minerals,[10,11] while $^{\bullet}OH$ produced upon oxidation of reduced HA was mainly by electron transfer from hydroquinones to O_2,

Received: May 26, 2022
Revised: September 28, 2022
Accepted: September 30, 2022

with H_2O_2 as an intermediate.[31] However, in soils and sediments, iron-containing minerals and SOM mutually interact, making it a complex process of ROS production. Yu et al. found that HA enhanced •OH production, which shifted the electron transfer pathway between solid Fe(II) and O_2.[27] Similarly, Zeng et al. reported that HA promoted •OH yield by complexing and dissolving Fe(II) from reduced clay minerals, which further efficiently reacted with H_2O_2 through a homogeneous pathway.[32] Except for HA, low-molecular-weight organic acids and thiols can complex with Fe(II), which facilitates •OH production upon oxygenation of siderite.[33] Notably, SOM is also the scavenger of •OH with the reaction rate constant to be $\sim 10^4$ L mg C^{-1} s^{-1}.[34] Zhang et al. showed that H-abstraction and •OH addition were the main reaction pathways between SOM and •OH, where the molecular weight, composition, functional groups, aromaticity, and saturation degree of SOM determined its reactivity with •OH.[35] Therefore, it is of interest whether different components of SOM promoted •OH yield or scavenged •OH, which would suppress its reaction with other substances during Fe(II) oxygenation. We posited that different SOM fractions, even the same fraction from different sources, may have different impacts on the yield of ROS as well as their production mechanism upon Fe(II) oxygenation, which have not been fully explored.

In turn, microbial iron reduction and ROS production also affect the transformation of SOM.[36] Under anoxic conditions, adsorbed SOM can be desorbed and dissolved as Fe(III) minerals are reduced,[37] with higher bioavailability that can serve as a carbon source for microorganisms and then be decomposed easily.[38−40] Under oxic conditions, dissolved organic matter (DOM) can react with the produced ROS, generate low-molecular-weight organic acids, and stimulate CO_2 emission.[27,35,41,42] SOM components are distinctly different, thus possessing DOM with diverse characteristics.[15] Still, the characteristics of dissolved fractions of FA, HA, and HM and their transformation after microbially mediated iron redox cycles remain unclear.

In this study, we employed a facultative anaerobic iron-reducing bacterium, *Shewanella oneidensis* MR-1, which remains active in redox cycles, along with the model iron mineral (i.e., ferrihydrite), and SOM fractions including FA, HA, and HM extracted from black soil and peat to (a) investigate the influence of SOM on microbial iron reduction and ROS production processes under fluctuating redox cycles, (b) reveal multiple production mechanisms of •OH in different SOM-containing systems and calculate the relative contributions of different pathways, and (c) explore the transformation of DOM after redox cycles. The results of this study will provide new insights into SOM-involved microbially mediated iron redox reactions.

MATERIALS AND METHODS

Materials. Black soil was collected from Heilongjiang, China (E 128°39′36″, N 47°43′12″), and Pahokee peat was obtained from the International Humic Substances Society (IHSS), both of which are of high organic carbon contents. Fulvic acid (FA), humic acid (HA), and humin (HM) were extracted from black soil (BFA, BHA, BHM) and peat (PFA, PHA, PHM). Procedures of extraction and electrochemical property analysis are presented in the Supporting Information (Texts S1 and S2, respectively). Characterization of samples is presented in the Supporting Information (Table S1). Ferrihydrite (Fh) was synthesized using the method reported in a previous study.[43] Characterization of Fh is shown in the Supporting Information (Table S2).

The dissimilatory iron-reducing bacterium, *Shewanella oneidensis* MR-1, was obtained from the American Type Culture Collection (ATCC, Manassas). Coumarin (COU, 99%) was purchased from Aladdin Bio-Chem Technology (Shanghai, China). Nitrotetrazolium blue chloride (NBT, 98%), 2,2′-bipyridine (BPY, 99%), and the hydroxylation product of COU, 7-hydroxycoumarin (7-hCOU, 98%) were purchased from J&K Scientific (Beijing, China). Catalase (CAT, from bovine liver, 2000−5000 units/mg) and bovine serum albumin (BSA, ≥ 98%) were obtained from Sigma-Aldrich (St. Louis, MO). Methanol (HPLC grade) was purchased from Macklin Biochemical Co., Ltd. (Shanghai, China). Other chemicals used in this study were of analytical grade. All containers were acid-washed and autoclaved before use.

Batch Experiment. *Shewanella oneidensis* MR-1 was incubated, harvested, washed, and resuspended in 0.1 M NaCl ($\sim 10^{10}$ cells/mL) according to the procedure previously reported.[11] All solutions were prepared with deoxygenated ultrapure water (18.2 MΩ/cm, Milli-Q system, Millipore) in a glovebox (Unilab Pro SP, MBraun, Germany) filled with high-purity N_2 (99.999%). A bicarbonate-buffered solution containing $NaHCO_3$, NH_4Cl, KCl, and KH_2PO_4 (pH 7.0),[11] Fh (1 g/L), *Shewanella oneidensis* MR-1 (10^8 cells/mL), lactate (10 mmol/L), and different types of soil organic matter (SOM, 100 mg C/L) were added to a 100 mL serum bottle in sequence. The bottles were settled overnight in the glovebox to remove trace oxygen. After that, they were capped with butyl rubber stoppers and moved to a shaker (150 r/min, 30 °C) outside the glovebox for incubation. After three days of anaerobic incubation, the butyl rubber stopper was changed to a sterile membrane, which blocked microorganism invasion but allowed air exchange, and then the bottles were placed in a shaker to incubate aerobically for one day. The whole reaction process was carried out in the dark. The bottles were subjected to four redox cycles, and the productions of dissolved and total Fe(II), as well as hydroxyl radicals (•OH), were determined at the end of each stage. Experimental groups without *Shewanella oneidensis* MR-1 or SOM or Fh were used as controls.

BPY, NBT, and CAT were used to evaluate the contribution of Fe(II), superoxide ($O_2^{\bullet-}$), and hydrogen peroxide (H_2O_2) on the production of •OH upon oxygenation in different SOM-containing systems, respectively.[11,44] Specifically, samples were collected at the end of the fifth anoxic phase where the bottles were incubated anaerobically for 30 days, and COU was also added to each sample in a glovebox. Then, 1 mmol/L BPY, 1 mmol/L NBT, and 1000 U/mL CAT were added to the samples respectively. The production of •OH upon oxidation in each system was determined. The relative contribution of $O_2^{\bullet-}$ and H_2O_2 was calculated by the decrease of •OH after the addition of complexing or quenching agents. All three agents were proved to have no influence on the determination of 7-hCOU (data not shown). All experiments were carried out in triplicate.

Measurements. The productions of dissolved and total Fe(II) were measured with the method reported in our previous study.[11] The content of solid-phase Fe(II) was calculated by subtracting dissolved Fe(II) from total Fe(II). The production of •OH was quantified using a fluorescent

https://doi.org/10.1021/acs.est.2c03799
Environ. Sci. Technol. XXXX, XXX, XXX−XXX

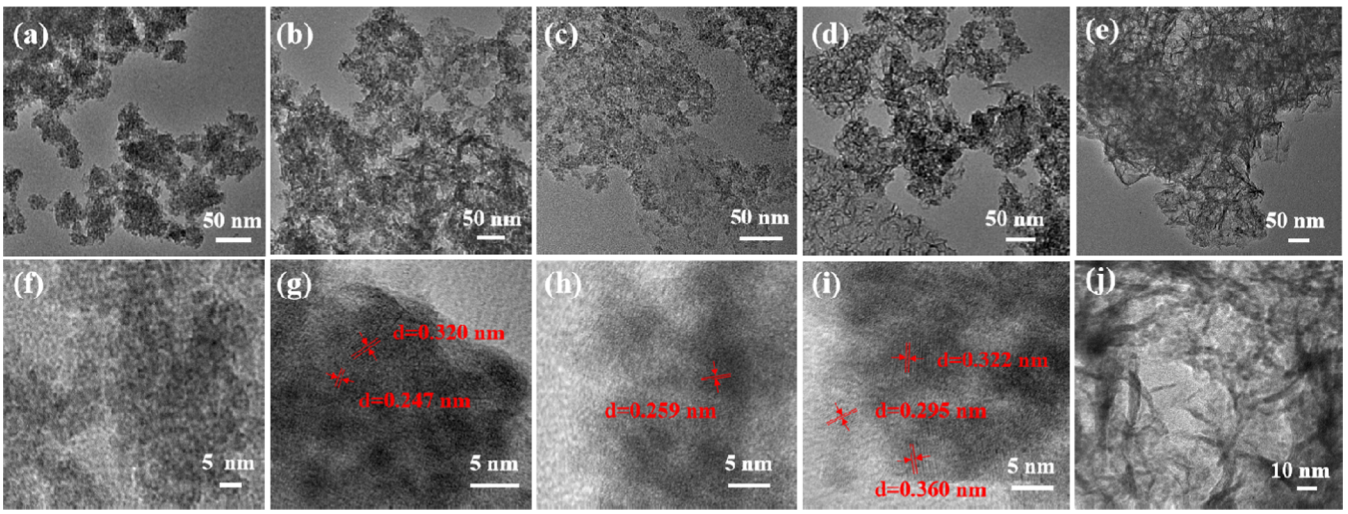

Figure 1. HRTEM spectra of ferrihydrite (a, f) and SOM-free (b, g), PFA- (c, h), PHA- (d, i), and PHM-containing systems (e, j) after microbially mediated redox cycles.

probe COU with an initial concentration of 1.5 mmol/L, which was mixed with 1 mL of collected samples (v/v, 1:1) and then exposed to air for 5 h oxygenation. After that, 0.5 mL of methanol was added to terminate the reaction, and the hydroxylated product of COU, 7-hCOU, was determined. The detection limit of 7-hCOU was 0.005 μmol/L. The concentration of $^{\bullet}$OH was calculated as [7-hCOU]/6.1%.[45] Although the concentration of COU was lower than that of HCO_3^- (30 mmol/L), the reaction rate constant of $^{\bullet}$OH with COU is 5.6×10^9 M^{-1} s^{-1},[46] three orders of magnitude higher than that with HCO_3^- (8.5×10^6 M^{-1} s^{-1}),[47,65] thus excluding the competition of HCO_3^- with COU to react with $^{\bullet}$OH, and the influence of lactate on $^{\bullet}$OH production was also ruled out (Figure S1).

Characterization of SOM, Fh, and Their Complexes. Supernatant in different SOM-containing systems was collected after microbially mediated iron redox cycles and filtered through a 0.22 μm filter to analyze the changes of DOM. UV−vis absorption spectra of DOM at wavelengths from 200 to 600 nm were measured by a UV−vis spectrophotometer (Specord250 Plus, Analytik Jena, Germany). The specific UV absorbance at 254 nm ($SUVA_{254}$) was calculated by normalizing the absorbance to the DOC concentration.[48] The fluorescence excitation−emission matrix (EEM) spectra were gathered by measuring the emission (Em) wavelengths from 250 to 550 nm at 2 nm increments and the excitation (Ex) wavelengths from 200 to 450 nm at 5 nm increments on a spectrofluorometer (F-4600, Hitachi, Japan). The photomultiplier tube voltage was set to 700 V at a scanning speed of 2400 nm/min. The contents of dissolved organic carbon were determined using a total organic carbon analyzer (vario TOC select, Elementar, Germany).

Synthesized Fh and samples after redox cycles were characterized using X-ray powder diffraction (XRD, Ultima IV, Rigaku, Japan). The phases were identified by comparing diffraction patterns with standard cards provided by the Joint Committee on Powder Diffraction Standards (JCPDS). The surface area of Fh was measured by the Brunauer−Emmett−Teller method (BET, ASAP 2460, Micromeritics) using nitrogen adsorption−desorption isotherm measurements at 77 K. For morphology analysis, the samples were taken after four redox cycles, dehydrated as previously described,[10] and characterized by scanning electron microscopy (SEM, Sigma 300, Zeiss, Germany) equipped with energy-dispersive X-ray spectroscopy (Smart EDX). Mineralogical characteristics of Fh were investigated using high-resolution transmission electron microscopy (HRTEM, JEM 200PLUS, JEOL, Japan).

Statistical Analysis. One-way analysis of variance (ANOVA) was performed to assess the differences among the data by Duncan post hoc comparisons at $p < 0.05$ using SPSS 22.0. Pearson correlations were calculated using the linear regression function in Origin 2018.

RESULTS AND DISCUSSION

Characterization of Organo−Mineral Complexes and Transformation of Fh after Redox Cycles. SEM was used to visualize the distribution of Fh and SOM, which may significantly affect the microbial Fe(III) reduction and ROS production processes. SOM can complex with iron, cover the surface of Fh, and form aggregates with Fh.[49−51] In the Fh sample, there were small particles aggregated with no crystalline structure (Figures S2a−c), consistent with the result of XRD (Figure S3). After being incubated with *Shewanella oneidensis* MR-1, there were large tabular minerals, compatible with vivianite,[52−54] surrounded by Fh aggregates (Figures S2d−f), which were also observed in the presence of HA (Figures S4d−f). The addition of FA showed the morphology of newly formed secondary minerals on the Fh surface (Figures S5c and S5f), while HA and HM were attached to Fh and formed big aggregates (Figures S4 and S6). This was consistent with the result of Zhou et al., who observed the aggregation of NOM and Fh in the microbe−Fh system with a high C/Fe ratio.[55]

To investigate the influence of SOM on the transformation of Fh, XRD and HRTEM were employed to characterize the minerals after redox cycles. Consistent with the result of SEM, in the Fh-only sample, particles with amorphous structure were aggregated (Figures 1a,f). After incubation with MR-1, vivianite (d = 0.320 nm, JCPDS No. 30-0662) and lepidocrocite (d = 0.247 nm, JCPDS No. 08-0098) were formed in the system without SOM (Figures 1g and S7a). The deposition of amorphous aggregated nanoparticles on Fh was also observed (Figure 1b), which promoted the growth of the surface phase and the formation of secondary minerals,

https://doi.org/10.1021/acs.est.2c03799
Environ. Sci. Technol. XXXX, XXX, XXX−XXX

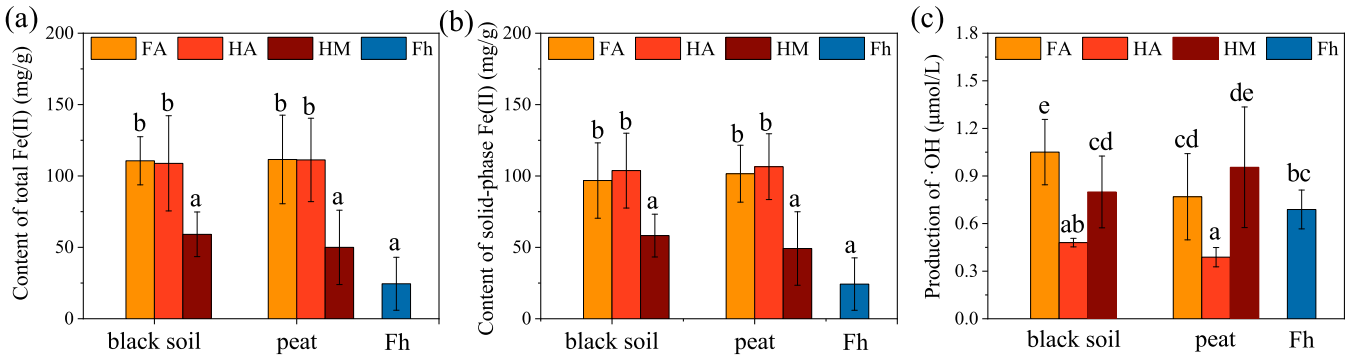

Figure 2. Production of total (a) and solid-phase Fe(II) (b) as well as •OH (c) in both SOM-free and SOM-containing systems. Different letters above bars indicate significant differences ($p < 0.05$) between different systems.

consistent with the phenomenon reported by Gomez et al.[56] FA induced the transformation of Fh to metavivianite (d = 0.259 nm, JCPDS No. 26-1137), while in the HA-containing system, secondary minerals including metavivianite (d = 0.295 nm), vivianite (d = 0.322 nm), and siderite (d = 0.360 nm, JCPDS No. 29-0696) were formed (Figures 1 and S7). In the HM-containing system, metavivianite was formed as confirmed by XRD analysis, while we only observed the coverage of HM on Fh in HRTEM spectra (Figures 1e,j and S7d). There were more vivianite and metavivianite formed rather than siderite, which was most likely due to the lower solubility product constant (K_{sp}) of vivianite ($Fe_3(PO_4)_2$) than that of siderite ($FeCO_3$, 1.3×10^{-22} and 3.13×10^{-11}, respectively). Unlike the results from the SOM-free system and our previous study where nanocrystallites including goethite, lepidocrocite, hematite, and vivianite were formed,[11] all of these newly formed minerals were ferrous minerals, indicating that HS may complex with Fe(II) and inhibit the transformation of secondary minerals to highly stable and crystalline iron oxy(hydr)oxides. Similar results indicated that organic carbon inhibited the transformation of Fh to more crystalline iron phases.[38,57,58] We speculated that it was because SOM complexed with both dissolved and adsorbed Fe(II), blocked fresh adsorption sites on the Fh surface, and thus prevented the adsorption of Fe(II), which further inhibited Fe(II)-catalyzed transformation of Fh.[38,59,60]

Production of Fe(II) and •OH in Different SOM-Containing Systems. The reaction systems were buffered with bicarbonate and the pH was around 7.0, which varied similarly as reported in our previous study under redox fluctuation.[11] Sustained production of Fe(II) was observed in SOM-containing systems during redox cycles (Figures S8a,b). The production of dissolved Fe(II) was in the range of 14.8−54.2 mg/g in FA- and HA-containing systems in the first anoxic phase (Figure S8c), suggesting that FA and HA promoted the generation of dissolved Fe(II), while in later redox cycles, it was lower than 4.4 mg/g, likely due to the adsorption of Fe(II) on stable organo−mineral complexes formed after the first redox cycle. FA and HA significantly promoted microbial iron reduction and increased the yield of total and solid-phase Fe(II) (Figures 2a,b). Although HM had no significant influence on the average yield of Fe(II) calculated from four redox cycles, the HM-containing system produced 1.2−10.2 times higher Fe(II) yield than the SOM-free system for each cycle. It may be due to the fact that FA and HA have higher EAC and EDC than HM, which acted as effective electron shuttles that promoted the electron transfer between Fh and MR-1 (Table S1).[61,62]

The yield of •OH was in the range of 0.4−1.4 μmol/L of samples collected from the anoxic phase upon oxygenation (Figures 2c and S8d). According to our previous study,[11] this concentration level of •OH could not cause damage or death of *Shewanella oneidensis* MR-1, and thus, the difference in bacterial quantity can be neglected. Although both FA and HA increased the yield of total Fe(II) up to almost five times, they had contrasting influences on the •OH production. Specifically, BFA promoted the yield of •OH and PFA had no significant influence on it, while HA significantly suppressed •OH yield. This was consistent with the fact that HA with a larger molecular size and a higher degree of unsaturation was more susceptible to •OH.[35] We speculated that HA with high EDC may compete with COU to react with •OH. To demonstrate this hypothesis, we employed a higher concentration of coumarin (10 mmol/L) to trap •OH. The results showed that the yield of •OH increased but was still lower than that in the SOM-free system (Figure S9), further confirming the high reaction rate of HA with •OH. In contrast to our results, Yu et al. reported that HA (20 or 40 mg C/L) enhanced the production of •OH during the oxygenation of reduced nontronite NAu-2, which increased as its EAC.[27] Therefore, we deduced that there was a dose−effect relationship that determined the role of HA in ROS production, and the source as well as composition of HA may also influence its effect on •OH production. Besides, there were nearly equal Fe(II) produced in two FA-containing systems, but the yield of •OH was significantly higher in BFA than that in the PFA system (Figure 2), indicating that the source of FA also affected the •OH production. The higher EDC of PFA than BFA may be a reason for the lower •OH yield. To explain the differences among different SOM-containing systems, the mechanisms for •OH production were further investigated.

Pathways for •OH Production in Different SOM-Containing Systems. According to previous studies, •OH could be produced through Fenton-like reactions and flavin-mediated pathways, which was secreted by *Shewanella oneidensis* MR-1 in microbe−mineral systems, with a small contribution of the latter process.[11,63] It has been proved that solid-phase Fe(II) rather than dissolved Fe(II) determined the production of •OH in our previous study.[11] To further explore the pathways of •OH production in SOM-containing systems, samples were collected at the end of the fifth anaerobic incubation phase. The yield of •OH produced upon oxygenation was measured with addition of various masking agents of

https://doi.org/10.1021/acs.est.2c03799
Environ. Sci. Technol. XXXX, XXX, XXX−XXX

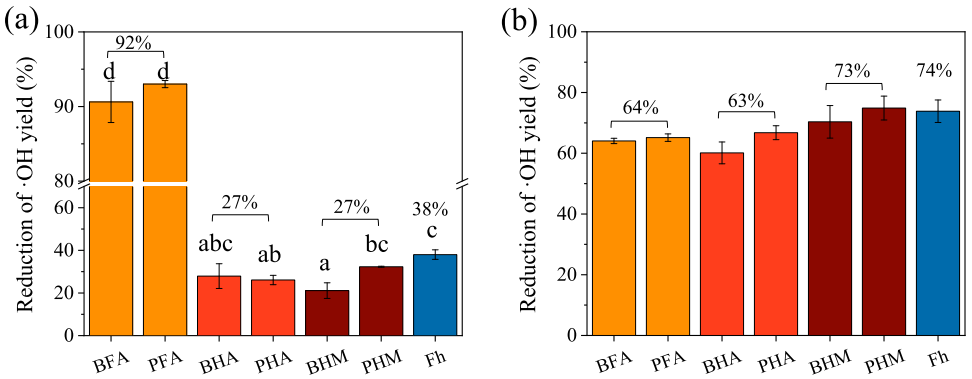

Figure 3. Reduction of •OH yield with the addition of 1 mmol/L NBT (a) and 1000 U/mL CAT (b) in different systems.

possible intermediates. BPY was widely used to screen Fe(II) in •OH production.[41,44,64] However, it should be noted that the reaction rate constant of BPY with •OH was 6.2×10^9 M^{-1} s^{-1},[65] which may compete with probes to consume •OH, thus resulting in the decrease of •OH yield. Therefore, we employed microbially reduced BFA and BHA, both of which contained negligible Fe(II), to verify the influence of BPY (1 mmol/L) on the trapping of •OH by COU (10 mmol/L). The yield of •OH produced upon oxygenation of reduced SOM was suppressed by 52−65% with the addition of BPY (Figure S10), suggesting that BPY competed intensely with COU to react with •OH, making it an unsuitable reagent to be used to evaluate the contribution of Fe(II) on •OH production.

In addition, excessive NBT was employed to evaluate its influence on •OH determination, and we found that higher NBT concentration had no influence on •OH yield (Figure S11), which means it can be used to determine the role of $O_2^{\bullet-}$ in •OH production. Then, 1 mmol/L NBT was added to scavenge $O_2^{\bullet-}$ and the yield of •OH was quantified. Interestingly, NBT suppressed over 90% of the yield of •OH in the FA-containing system, whereas it only reduced 20−38% of •OH yield in other systems (Figure 3a). It is thus presumed that $O_2^{\bullet-}$ was the most important intermediate of •OH production in the FA-containing system and a minor participant in other systems. Furthermore, CAT was used to explore the role of H_2O_2 in •OH production. To test the specificity of CAT to scavenge H_2O_2 and whether it reacted with •OH, we added excess CAT (1000, 1250, 1500 U/mL) to microbially reduced Fh-SOM samples before being exposed to air for oxygenation and found that excessive CAT did not suppress more •OH (Figure S12a). Bovine serum albumin (BSA) was also added to the reduced samples for oxygenation and •OH was not significantly influenced (Figure S12b), which further suggested that •OH did not react with amino acids at the CAT surface. These results were consistent with previous studies that CAT was an effective quencher of H_2O_2 but could not react with •OH.[31,66] The addition of 1000 U/mL CAT suppressed 60−75% of •OH yields in all systems (Figure 3b), indicating that H_2O_2 was a crucial intermediate in •OH production. Compared to HA and HM, FA is soluble with smaller molecular size and higher oxygen-containing groups, which efficiently mediated electron transfer between solid-phase Fe(II) and O_2, leading to a one-electron transfer process for •OH production, whereas HA and HM mainly present as particles, which adsorbed, aggregated, and covered the Fh surface, making the oxidation reaction more complex. It might involve many processes, including accepting electrons from Fe(II), transferring electron transfer to oxygen, inhibiting contact between Fe(II) and O_2, and thus resulting in both one- and two-electron transfer processes.

Except for Fe(II)-mediated pathway, reduced SOM can also contribute to •OH production. Therefore, we further used microbially reduced SOM to investigate the production of •OH during the oxidation process. As shown in Figure S13, SOM can act as a rechargeable battery under fluctuating redox conditions, which was reduced by *Shewanella oneidensis* MR-1 under anoxic conditions and then oxidized and produced •OH under oxic conditions. However, the same SOM fraction from different sources showed totally different capacities in •OH production, especially for FA and HA, whereas HM is less redox-active and •OH produced was negligible. We further employed $O_2^{\bullet-}$ quencher NBT and H_2O_2 decomposer CAT to explore the involvements of intermediates $O_2^{\bullet-}$ and H_2O_2, both of which were proved as specific and efficient masking agents.[67,68] The results showed that NBT reduced over 72% of •OH production in microbially mediated FA and HA systems (Figure S14a), suggesting that reduced FA and HA preferentially transferred one electron to O_2 and formed $O_2^{\bullet-}$. The addition of 1000 U/mL CAT to FA and HA systems reduced over 96% of •OH yield (Figure S14b), which means that H_2O_2 was the essential intermediate in •OH production by oxidation of reduced SOM. These results implied that the one-electron transfer process dominated •OH production during the oxidation of microbially reduced FA and HA. This was opposite to the two-electron transfer process from reduced HA to O_2 reported by Yu et al.[27] We assumed that it was because microbially reduced solid HA was employed in this study, while chemically reduced dissolved HA was used by Yu et al., and such different reduction methods and phase states of HA affected redox-active functional groups and the electron exchange capacity (EEC) of reduced HA.[18,31] Besides, semiquinone has been proven to reduce O_2 to $O_2^{\bullet-}$ and further dismutate to H_2O_2 and O_2, which supports a one-electron transfer process for •OH production.[69]

In summary, chemical oxidation of Fe(II) produced by dissimilatory iron-reducing bacteria dominated the production of •OH, and the oxidation of microbially reduced SOM also contributed to •OH production (Figure 4). In the FA-containing system, $O_2^{\bullet-}$ was the vital intermediate, which indicated that •OH was mainly produced by the one-electron transfer mechanism. In HA- and HM-containing and SOM-free systems, $O_2^{\bullet-}$ and H_2O_2 contributed to •OH production by 27−38% and 63−74%, respectively, demonstrating that one-

https://doi.org/10.1021/acs.est.2c03799
Environ. Sci. Technol. XXXX, XXX, XXX−XXX

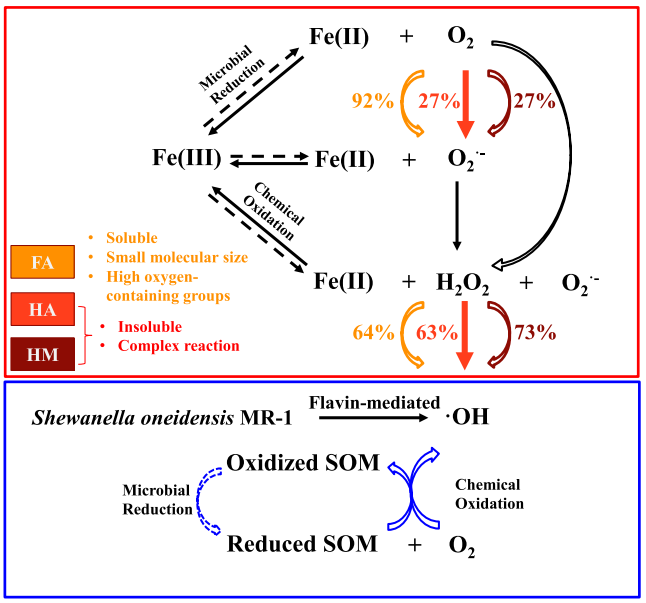

Figure 4. Schematic diagram of the pathway for •OH production in different SOM-containing systems.

and two-electron transfer processes happened simultaneously. Similar results were reported that both one- and two-electron transfer processes were present during the oxygenation of iron (oxyhydr)oxides as well as reduced clay mineral with the presence of HA.[11,27] In addition, •OH can also be generated through flavin-mediated and maybe other unexplored pathways without the involvement of H_2O_2.[63]

Effect of Microbially Mediated Redox Cycles on DOM Optical Characteristics. The characteristics of DOM in different SOM-containing systems before and after four redox cycles were investigated using a total organic carbon analyzer and UV−vis and fluorescence spectrophotometers. Although Fourier transform ion cyclotron resonance mass spectrometry (FT-ICR-MS) is a powerful tool to identify the molecular composition of organic matter, it is not appropriate for HA fractions that have high contents of aromatics and are easy to aggregate. The DOC concentration of three kinds of SOM followed the order FA > HA > HM (Table S3) because of the operational definition that FA is soluble at all pH conditions.[70] The DOC concentration was higher in the SOM-Fh system than that in the pure SOM solution due to the addition of lactate and the SOM-Fh-MR-1 system, since MR-1 consumed lactate and part of DOM, which can also be degraded by produced ROS. The aromaticity derived from the $SUVA_{254}$ of DOM followed the order HA > FA > HM (Table S3). With the addition of Fh, the aromaticity of DOM was severely reduced mainly because of the adsorption of aromatic molecules on minerals.[43,71] Further incubation with *Shewanella oneidensis* MR-1 induced different changes in aromaticity. The aromaticity of DOM was increased in FA- and HM-containing microbe−mineral systems compared to the system without *Shewanella oneidensis* MR-1, which was probably due to the secretion of aromatics such as flavin and other aromatic extracellular polymeric substances (EPS) by *Shewanella oneidensis* MR-1. The release of aromatic substances during the transformation of Fh also contributed to the increase of $SUVA_{254}$.[38] While in the HA-containing system, the results were reversed. This was consistent with the above results that the higher EDC of HA led to its higher reactivity with •OH and resulted in the low aromaticity of DOM.

We further investigated the fluorescent characteristics of DOM. The dissolved fraction of each kind of SOM from two different sources showed similar fluorescent characteristics (Figure S15a−c,g−i). *Shewanella oneidensis* MR-1 produced fluorescent components including aromatic protein II (E_x/E_m = 220/345 nm), aromatic protein I (E_x/E_m = 225/330 nm), and soluble microbial byproduct-like substance (E_x/E_m = 275/345, Figure S15m), which can be attributed to its EPS.[72] In the HA-containing microbe−mineral system, there were three peaks belonging to EPS and humic acid (E_x/E_m = 285/415 nm, Figure S15e,k), which was slightly different from the pristine HA (E_x/E_m = 265/430 nm) and may be transformed by produced •OH.[32] EPS and humic acid-like substances (E_x/E_m = 255−345/420−430 nm) were also detected in both FA- and HM-containing microbe−mineral systems after redox cycles (Figures S15). In fact, in the microbe−mineral system, SOM experienced complex processes. During microbial iron reduction, adsorbed OM was released partly and *Shewanella oneidensis* MR-1 may utilize it to produce new metabolites.[1,36] Under oxic conditions, DOM may coprecipitate with iron or readsorb on newly formed secondary mineral, and part of DOM may react with •OH, which can even be decomposed to CO_2.[32,35] Therefore, the results presented here just provided general information about DOM optical characteristics after redox cycles and further investigation is still needed.

Environmental Implications. Microbially mediated iron redox cycling strongly affects the fate of pollutants and the biogeochemical cycle of nutrient elements in the soil environment, which is influenced by SOM. This is the first study to investigate the influence of different SOM components on microbial iron reduction and oxidation processes. Under anoxic conditions, FA and HA promoted the production of Fe(II) by acting as electron shuttles due to their high EAC and EDC. Upon oxygenation, HA inhibited the yield of •OH because of its high EDC where it can react with the produced •OH more efficiently. Additionally, the mechanisms for •OH production in different SOM-containing systems were different. The one-electron transfer process dominated the •OH production in the FA-containing system, while both one- and two-electron transfer processes were present in HA- and HM-containing as well as SOM-free systems. After iron redox cycles, the aromaticity of DOM of HA decreased, while it increased for FA and HM. However, the behavior of DOM during the redox cycle is complex, including adsorption and desorption of DOM, utilization, degradation, and production by microbes, and oxidation by ROS. The dynamics and mechanisms of carbon circulation can be further investigated using isotope labeling and high-resolution in situ characterization techniques such as nanoscale secondary ion mass spectrometry (Nano-SIMS) and atomic force microscopy combined with Fourier transform infrared spectroscopy (AFM-FTIR).

This study is helpful to understand the microbial iron reduction and ROS production processes in oxygen-fluctuated soil environments such as paddy soil, wetland, and subsurface with a fluctuating water table, since the system established here is much closer to the real environment. Different C/Fe ratios have been reported that influenced the reduction extent of Fh,[55] which may further affect ROS production. The result here about the effect of HA on ROS production is opposite to previous studies,[27,32] and thus, we deduce that there is a dose−

https://doi.org/10.1021/acs.est.2c03799
Environ. Sci. Technol. XXXX, XXX, XXX−XXX

effect relationship that determines the role of SOM in ROS production, which still needs to be proved. The source of SOM may be another factor influencing the process. Actually, the content and composition of SOM in soils varied significantly. Therefore, it is necessary to consider these properties of SOM when evaluating SOM-affecting iron reduction and ROS production processes, especially in soils with high SOM contents. For example, SOM with high EDC may largely compete with reduced pollutants to react with •OH, thus reducing its effect on contaminant degradation. As the humic fertilizer has become a common soil amendment,[73] this study provides valuable information for its potential impact on the behavior of both nutrients and pollutants.

■ ASSOCIATED CONTENT

Supporting Information

The Supporting Information is available free of charge at https://pubs.acs.org/doi/10.1021/acs.est.2c03799.

Extraction procedures, electrochemical analysis, and elemental composition of SOM; surface characteristics of Fh; DOM characterization; XRD and SEM spectra of Fh, SOM-free and SOM-containing microbe−mineral systems; production of Fe(II) and •OH during redox cycles; •OH produced by microbially reduced SOM with and without scavengers; influences of lactate, BPY, NBT, CAT, and higher concentration of COU on •OH production; and fluorescence spectra of DOM before and after redox cycles (PDF)

■ AUTHOR INFORMATION

Corresponding Author

Gang Li − *Key Laboratory of Urban Environment and Health, Ningbo Urban Environment Observation and Research Station, Institute of Urban Environment, Chinese Academy of Sciences, Xiamen 361021, China; Zhejiang Key Laboratory of Urban Environmental Processes and Pollution Control, CAS Haixi Industrial Technology Innovation Center in Beilun, Ningbo 315830, China;* orcid.org/0000-0002-1674-4587; Email: gli@iue.ac.cn

Authors

Ruixia Han − *Key Laboratory of Urban Environment and Health, Ningbo Urban Environment Observation and Research Station, Institute of Urban Environment, Chinese Academy of Sciences, Xiamen 361021, China; CAS Key Laboratory of Soil Environment and Pollution Remediation, Institute of Soil Science, Chinese Academy of Sciences, Nanjing 210008, China; Zhejiang Key Laboratory of Urban Environmental Processes and Pollution Control, CAS Haixi Industrial Technology Innovation Center in Beilun, Ningbo 315830, China*

Zhe Wang − *Key Laboratory of Urban Environment and Health, Ningbo Urban Environment Observation and Research Station, Institute of Urban Environment, Chinese Academy of Sciences, Xiamen 361021, China; Zhejiang Key Laboratory of Urban Environmental Processes and Pollution Control, CAS Haixi Industrial Technology Innovation Center in Beilun, Ningbo 315830, China*

Jitao Lv − *State Key Laboratory of Environmental Chemistry and Ecotoxicology, Research Center for Eco-Environmental Sciences, Chinese Academy of Sciences, Beijing 100085, China;* orcid.org/0000-0002-5664-0029

Zhe Zhu − *Key Laboratory of Urban Environment and Health, Ningbo Urban Environment Observation and Research Station, Institute of Urban Environment, Chinese Academy of Sciences, Xiamen 361021, China; Zhejiang Key Laboratory of Urban Environmental Processes and Pollution Control, CAS Haixi Industrial Technology Innovation Center in Beilun, Ningbo 315830, China; Department of Chemical and Environmental Engineering, Faculty of Science and Engineering, University of Nottingham, Ningbo 315100, China*

Guang-Hui Yu − *Institute of Surface-Earth System Science, School of Earth System Science, Tianjin University, Tianjin 300072, China;* orcid.org/0000-0002-5699-779X

Yong-Guan Zhu − *Key Laboratory of Urban Environment and Health, Ningbo Urban Environment Observation and Research Station, Institute of Urban Environment, Chinese Academy of Sciences, Xiamen 361021, China; Zhejiang Key Laboratory of Urban Environmental Processes and Pollution Control, CAS Haixi Industrial Technology Innovation Center in Beilun, Ningbo 315830, China; State Key Laboratory of Environmental Chemistry and Ecotoxicology, Research Center for Eco-Environmental Sciences, Chinese Academy of Sciences, Beijing 100085, China;* orcid.org/0000-0003-3861-8482

Complete contact information is available at: https://pubs.acs.org/10.1021/acs.est.2c03799

Notes

The authors declare no competing financial interest.

■ ACKNOWLEDGMENTS

This work was funded by the National Natural Science Foundation of China (42107014), Ningbo Bureau of Science and Technology (2021Z101), the National Postdoctoral Program for Innovative Talents (BX2021292), the China Postdoctoral Science Foundation (2021M693112), and the grants from CAS Key Laboratory of Soil Environment and Pollution Remediation, Institute of Soil Science, Chinese Academy of Sciences (SEPR2020-01).

■ REFERENCES

(1) Yu, C.; Xie, S.; Song, Z.; Xia, S.; Åström, M. E. Biogeochemical cycling of iron (hydr-)oxides and its impact on organic carbon turnover in coastal wetlands: A global synthesis and perspective. *Earth-Sci. Rev.* **2021**, *218*, No. 103658.

(2) Borch, T.; Kretzschmar, R.; Kappler, A.; Cappellen, P. V.; Ginder-Vogel, M.; Voegelin, A.; Campbell, K. Biogeochemical redox processes and their impact on contaminant dynamics. *Environ. Sci. Technol.* **2010**, *44*, 15−23.

(3) Kappler, A.; Bryce, C.; Mansor, M.; Lueder, U.; Byrne, J. M.; Swanner, E. D. An evolving view on biogeochemical cycling of iron. *Nat. Rev. Microbiol.* **2021**, *19*, 360−374.

(4) Shi, L.; Dong, H.; Reguera, G.; Beyenal, H.; Lu, A.; Liu, J.; Yu, H. Q.; Fredrickson, J. K. Extracellular electron transfer mechanisms between microorganisms and minerals. *Nat. Rev. Microbiol.* **2016**, *14*, 651−662.

(5) Hartshorne, R. S.; Reardonb, C. L.; Rossc, D.; Nuesterd, J.; Clarkea, T. A.; Gatesa, A. J.; Millsa, P. C.; Fredricksonb, J. K.; Zacharab, J. M.; Shib, L.; Beliaevb, A. S.; Marshallb, M. J.; Tienc, M.; Brantleyd, S.; Butta, J. N.; Richardsona, D. J. Characterization of an electron conduit between bacteria and the extracellular environment. *Proc. Natl. Acad. Sci. U.S.A.* **2009**, *106*, 22169−22174.

(6) Gorby, Y. A.; Yanina, S.; McLean, J. S.; Rosso, K. M.; Moyles, D.; Dohnalkova, A.; Beveridge, T. J.; Chang, I. S.; Kim, B. H.; Kim, K. S.; Culley, D. E.; Reed, S. B.; Romine, M. F.; Saffarini, D. A.; Hill, E.

A.; Shi, L.; Elias, D. A.; Kennedy, D. W.; Pinchuk, G.; Watanabe, K.; Ishii, Si.; Logan, B.; Nealson, K. H.; Fredrickson, J. K. Electrically conductive bacterial nanowires produced by Shewanella oneidensis strain MR-1 and other microorganisms. *Proc. Natl. Acad. Sci. U.S.A.* **2006**, *103*, 11358−11363.
(7) Hu, S.; Wu, Y.; Li, F.; Shi, Z.; Ma, C.; Liu, T. Fulvic Acid-Mediated Interfacial Reactions on exposed hematite facets during dissimilatory iron reduction. *Langmuir* **2021**, *37*, 6139−6150.
(8) Cutting, R. S.; Coker, V. S.; Fellowes, J. W.; Lloyd, J. R.; Vaughan, D. J. Mineralogical and morphological constraints on the reduction of Fe(III) minerals by Geobacter sulfurreducens. *Geochim. Cosmochim. Acta* **2009**, *73*, 4004−4022.
(9) Bose, S.; Hochella, M. F.; Gorby, Y. A.; Kennedy, D. W.; McCready, D. E.; Madden, A. S.; Lower, B. H. Bioreduction of hematite nanoparticles by the dissimilatory iron reducing bacterium *Shewanella oneidensis* MR-1. *Geochim. Cosmochim. Acta* **2009**, *73*, 962−976.
(10) Han, R.; Lv, J.; Zhang, S.; Zhang, S. Hematite facet-mediated microbial dissimilatory iron reduction and production of reactive oxygen species during aerobic oxidation. *Water Res.* **2021**, *195*, No. 116988.
(11) Han, R.; Lv, J.; Huang, Z.; Zhang, S.; Zhang, S. Pathway for the production of hydroxyl radicals during the microbially mediated redox transformation of iron (oxyhydr)oxides. *Environ. Sci. Technol.* **2020**, *54*, 902−910.
(12) Kleber, M.; Bourg, I. C.; Coward, E. K.; Hansel, C. M.; Myneni, S. C. B.; Nunan, N. Dynamic interactions at the mineral−organic matter interface. *Nat. Rev. Earth Environ.* **2021**, *2*, 402−421.
(13) Wander, M. M.; Traina, S. J. Organic fractions from organically and conventionally managed soils: II. Characterization of composition. *Soil Sci. Soc. Am. J.* **1996**, *60*, 1087−1094.
(14) Stevenson, F. J. *Humus Chemistry: Genesis, Composition, Reactions*; John Wiley & Sons: New York, 1994.
(15) Schellekens, J.; Buurman, P.; Kalbitz, K.; Zomeren, A. V.; Vidal-Torrado, P.; Cerli, C.; Comans, R. N. Molecular features of humic acids and fulvic acids from contrasting environments. *Environ. Sci. Technol.* **2017**, *51*, 1330−1339.
(16) Sheng, Y.; Dong, H.; Kukkadapu, R. K.; Ni, S.; Zeng, Q.; Hu, J.; Coffin, E.; Zhao, S.; Sommer, A. J.; McCarrick, R. M.; Lorigan, G. A. Lignin-enhanced reduction of structural Fe(III) in nontronite: Dual roles of lignin as electron shuttle and donor. *Geochim. Cosmochim. Acta* **2021**, *307*, 1−21.
(17) Stern, N.; Mejia, J.; He, S.; Yang, Y.; Ginder-Vogel, M.; Roden, E. E. Dual role of humic substances as electron donor and shuttle for dissimilatory iron reduction. *Environ. Sci. Technol.* **2018**, *52*, 5691−5699.
(18) Klüpfel, L.; Piepenbrock, A.; Kappler, A.; Sander, M. Humic substances as fully regenerable electron acceptors in recurrently anoxic environments. *Nat. Geosci.* **2014**, *7*, 195−200.
(19) Scott, D. T.; Mcknight, D. M.; Blunt-Harris, E. L.; Kolesar, S. E.; Lovley, D. R. Quinone moieties act as electron acceptors in the reduction of humic substances by humics-reducing microorganisms. *Environ. Sci. Technol.* **1998**, *32*, 2984−2989.
(20) Lovley, D. R.; Fraga, J. L.; Blunt-Harris, E. L.; Hayes, L. A.; Phillips, E. J. P.; Coates, J. D. Humic substances as a mediator for microbially catalyzed metal reduction. *Acta Hydrochim. Hydrobiol.* **1998**, *26*, 152−157.
(21) Roden, E. E.; Kappler, A.; Bauer, I.; Jiang, J.; Paul, A.; Stoesser, R.; Konishi, H.; Xu, H. Extracellular electron transfer through microbial reduction of solid-phase humic substances. *Nat. Geosci.* **2010**, *3*, 417−421.
(22) Yang, C.; Hou, L.-X.; Xi, B.-D.; Hou, L.-A.; He, X.-S. Contribution of redox-active properties of compost-derived humic substances in hematite bioreduction. *Chin. Chem. Lett.* **2022**, *33*, 2731−2735.
(23) Yang, P.; Jiang, T.; Cong, Z.; Liu, G.; Guo, Y.; Liu, Y.; Shi, J.; Hu, L.; Yin, Y.; Cai, Y.; Jiang, G. Loss and increase of the electron exchange capacity of natural organic matter during its reduction and reoxidation: The role of quinone and nonquinone moieties. *Environ. Sci. Technol.* **2022**, *56*, 6744−6753.
(24) Hu, S.; Wu, Y.; Shi, Z.; Li, F.; Liu, T. Quinone-mediated dissimilatory iron reduction of hematite: Interfacial reactions on exposed {001} and {100} facets. *J. Colloid Interface Sci.* **2021**, *583*, 544−552.
(25) Bai, Y.; Sun, T.; Angenent, L. T.; Haderlein, S. B.; Kappler, A. Electron hopping enables rapid electron transfer between quinone-/hydroquinone-containing organic molecules in microbial iron(III) mineral reduction. *Environ. Sci. Technol.* **2020**, *54*, 10646−10653.
(26) Bai, Y.; Mellage, A.; Cirpka, O. A.; Sun, T.; Angenent, L. T.; Haderlein, S. B.; Kappler, A. AQDS and redox-active NOM enables microbial Fe(III)-mineral reduction at cm-scales. *Environ. Sci. Technol.* **2020**, *54*, 4131−4139.
(27) Yu, C.; Zhang, Y.; Lu, Y.; Qian, A.; Zhang, P.; Cui, Y.; Yuan, S. Mechanistic insight into humic acid-enhanced hydroxyl radical production from Fe(II)-bearing clay mineral oxygenation. *Environ. Sci. Technol.* **2021**, *55*, 13366−13375.
(28) Xie, W.; Yuan, S.; Tong, M.; Ma, S.; Liao, W.; Zhang, N.; Chen, C. Contaminant degradation by *OH during sediment oxygenation: Dependence on Fe(II) species. *Environ. Sci. Technol.* **2020**, *54*, 2975−2984.
(29) Liao, P.; Yu, K.; Lu, Y.; Wang, P.; Liang, Y.; Shi, Z. Extensive dark production of hydroxyl radicals from oxygenation of polluted river sediments. *Chem. Eng. J.* **2019**, *368*, 700−709.
(30) Page, S. E.; Kling, G. W.; Sander, M.; Harrold, K. H.; Logan, J. R.; McNeill, K.; Cory, R. M. Dark formation of hydroxyl radical in Arctic soil and surface waters. *Environ. Sci. Technol.* **2013**, *47*, 12860−12867.
(31) Page, S. E.; Sander, M.; Arnold, W. A.; McNeill, K. Hydroxyl radical formation upon oxidation of reduced humic acids by oxygen in the dark. *Environ. Sci. Technol.* **2012**, *46*, 1590−1597.
(32) Zeng, Q.; Wang, X.; Liu, X.; Huang, L.; Hu, J.; Chu, R. K.; Tolic, N.; Dong, H. Mutual interactions between reduced Fe-bearing clay minerals and humic acids under dark, oxygenated condition: hydroxyl radical generation and humic acid transformation. *Environ. Sci. Technol.* **2020**, *54*, 15013−15023.
(33) Yu, H.; Zhang, P.; Liu, J.; Zheng, Y.; Mustapha, N. A. Effects of low-molecular-weight organic acids/thiols on hydroxyl radical production from natural siderite oxidation. *Chem. Geol.* **2021**, *584*, No. 120537.
(34) Westerhoff, P.; Mezyk, S. P.; Cooper, W. J.; Minakata, D. Electron pulse radiolysis determination of hydroxyl radical rate constants with Suwannee River fulvic acid and other dissolved organic matter isolates. *Environ. Sci. Technol.* **2007**, *41*, 4640−4646.
(35) Zhang, S.; Hao, Z.; Liu, J.; Gutierrez, L.; Croué, J.-P. Molecular insights into the reactivity of aquatic natural organic matter towards hydroxyl (•OH) and sulfate ($SO_4^{\bullet-}$) radicals using FT-ICR MS. *Chem. Eng. J.* **2021**, *425*, No. 130622.
(36) Hu, J.; Zeng, Q.; Chen, H.; Dong, H. Effect of bacterial cell addition on Fe(III) reduction and soil organic matter transformation in a farmland soil. *Geochim. Cosmochim. Acta* **2022**, *325*, 25−38.
(37) Pan, W.; Kan, J.; Inamdar, S.; Chen, C.; Sparks, D. Dissimilatory microbial iron reduction release DOC (dissolved organic carbon) from carbon-ferrihydrite association. *Soil Biol. Biochem.* **2016**, *103*, 232−240.
(38) Adhikari, D.; Zhao, Q.; Das, K.; Mejia, J.; Huang, R.; Wang, X.; Poulson, S. R.; Tang, Y.; Roden, E. E.; Yang, Y. Dynamics of ferrihydrite-bound organic carbon during microbial Fe reduction. *Geochim. Cosmochim. Acta* **2017**, *212*, 221−233.
(39) Chen, C.; Hall, S. J.; Coward, E.; Thompson, A. Iron-mediated organic matter decomposition in humid soils can counteract protection. *Nat. Commun.* **2020**, *11*, No. 2255.
(40) Zeng, Q.; Huang, L.; Ma, J.; Zhu, Z.; He, C.; Shi, Q.; Liu, W.; Wang, X.; Xia, Q.; Dong, H. Bio-reduction of ferrihydrite-montmorillonite-organic matter complexes: Effect of montmorillonite and fate of organic matter. *Geochim. Cosmochim. Acta* **2020**, *276*, 327−344.

https://doi.org/10.1021/acs.est.2c03799
Environ. Sci. Technol. XXXX, XXX, XXX−XXX

(41) Chen, N.; Fu, Q.; Wu, T.; Cui, P.; Fang, G.; Liu, C.; Chen, C.; Liu, G.; Wang, W.; Wang, D.; Wang, Pa.; Zhou, D. Active iron phases regulate the abiotic transformation of organic carbon during redox fluctuation cycles of paddy soil. *Environ. Sci. Technol.* **2021**, *55*, 14281−14293.
(42) Tan, M.; Liu, S.; Chen, N.; Li, Y.; Ge, L.; Zhu, C.; Zhou, D. Hydroxyl radicals induced mineralization of organic carbon during oxygenation of ferrous mineral-organic matter associations: Adsorption versus coprecipitation. *Sci. Total Environ.* **2021**, No. 151667.
(43) Lv, J.; Zhang, S.; Wang, S.; Luo, L.; Cao, D.; Christie, P. Molecular-scale investigation with ESI-FT-ICR-MS on fractionation of dissolved organic matter induced by adsorption on iron oxyhydroxides. *Environ. Sci. Technol.* **2016**, *50*, 2328−2336.
(44) Tong, M.; Yuan, S.; Ma, S.; Jin, M.; Liu, D.; Cheng, D.; Liu, X.; Gan, Y.; Wang, Y. Production of abundant hydroxyl radicals from oxygenation of subsurface sediments. *Environ. Sci. Technol.* **2016**, *50*, 214−221.
(45) Žerjav, G.; Albreht, A.; Vovk, I.; Pintar, A. Revisiting terephthalic acid and coumarin as probes for photoluminescent determination of hydroxyl radical formation rate in heterogeneous photocatalysis. *Appl. Catal., A* **2020**, *598*, No. 117566.
(46) Rutely C, B. C.; Jean-M, F.; Walter, T. Z.; Xochitl, D. B.; Mika, S. Towards reliable quantification of hydroxyl radicals in the Fenton reaction using chemical probes. *RSC Adv.* **2018**, *8*, 5321−5330.
(47) Gligorovski, S.; Strekowski, R.; Barbati, S.; Vione, D. Environmental implications of hydroxyl radicals (•OH). *Chem. Rev.* **2015**, *115*, 13051−13092.
(48) Weishaar, J. L.; Aiken, G. R.; Bergamaschi, B. A.; Fram, M. S.; Fujii, R.; Mopper, K. Evaluation of specific ultraviolet absorbance as an indicator of the chemical composition and reactivity of dissolved organic carbon. *Environ. Sci. Technol.* **2003**, *37*, 4702−4708.
(49) Chen, K.-Y.; Chen, T.; Chan, Y.; Cheng, C.; Tzou, Y.; Liu, Y.; Teah, H. Stabilization of natural organic matter by short-range-order iron hydroxides. *Environ. Sci. Technol.* **2016**, *50*, 12612−12620.
(50) Chen, C.; Dynes, J. J.; Wang, J.; Karunakaran, C.; Sparks, D. L. Soft X-ray spectromicroscopy study of mineral-organic matter associations in pasture soil clay fractions. *Environ. Sci. Technol.* **2014**, *48*, 6678−6686.
(51) Poggenburg, C.; Mikutta, R.; Schippers, A.; Dohrmann, R.; Guggenberger, G. Impact of natural organic matter coatings on the microbial reduction of iron oxides. *Geochim. Cosmochim. Acta* **2018**, *224*, 223−248.
(52) Muehe, E. M.; Morin, G.; Scheer, L.; Pape, P. L.; Esteve, I.; Daus, B.; Kappler, A. Arsenic(V) incorporation in vivianite during microbial reduction of arsenic(V)-bearing biogenic Fe(III) (oxyhydr)oxides. *Environ. Sci. Technol.* **2016**, *50*, 2281−2291.
(53) Sánchez-Román, M.; Puente-Sanchez, F.; Parro, V.; Amils, R. Nucleation of Fe-rich phosphates and carbonates on microbial cells and exopolymeric substances. *Front. Microbiol.* **2015**, *6*, No. 1024.
(54) Notini, L.; Byrne, J. M.; Tomaszewski, E.; Latta, D. E.; Zhou, Z.; Scherer, M. M.; Kappler, A. Mineral defects enhance bioavailability of goethite towards microbial Fe(III) reduction. *Environ. Sci. Technol.* **2019**, *53*, 8883−8891.
(55) Zhou, Z.; Muehe, E. M.; Tomaszewski, E. J.; Lezama-Pacheco, J.; Kappler, A.; Byrne, J. M. Effect of natural organic matter on the fate of cadmium during microbial ferrihydrite reduction. *Environ. Sci. Technol.* **2020**, *54*, 9445−9453.
(56) Gomez, M. A.; Jiang, R.; Song, M.; Li, D.; Lea, A. S.; Ma, X.; Wang, H.; Yin, X.; Wang, S.; Jia, Y. Further insights into the Fe(II) reduction of 2-line ferrihydrite: a semi in situ and in situ TEM study. *Nanoscale Adv.* **2020**, *2*, 4938−4950.
(57) Yu, W.; Chu, C.; Chen, B. Enhanced microbial ferrihydrite reduction by pyrogenic carbon: Impact of graphitic structures. *Environ. Sci. Technol.* **2022**, *56*, 239−250.
(58) Chen, C.; Thompson, A. The influence of native soil organic matter and minerals on ferrous iron oxidation. *Geochim. Cosmochim. Acta* **2021**, *292*, 254−270.
(59) Xiao, W.; Jones, A. M.; Li, X.; Collins, R. N.; Waite, T. D. Effect of Shewanella oneidensis on the kinetics of Fe(II)-catalyzed transformation of ferrihydrite to crystalline iron oxides. *Environ. Sci. Technol.* **2018**, *52*, 114−123.
(60) Sheng, A.; Liu, J.; Li, X.; Qafoku, O.; Collins, R. N.; Jones, A. M.; Pearce, C. I.; Wang, C.; Ni, J.; Lu, A.; Rosso, K. M. Labile Fe(III) from sorbed Fe(II) oxidation is the key intermediate in Fe(II)-catalyzed ferrihydrite transformation. *Geochim. Cosmochim. Acta* **2020**, *272*, 105−120.
(61) Fritzsche, A.; Bosch, J.; Sander, M.; Schröder, C.; Byrne, J. M.; Ritschel, T.; Joshi, P.; Maisch, M.; Meckenstock, R. U.; Kappler, A.; Totsche, K. U. Organic matter from redoximorphic soils accelerates and sustains microbial Fe(III) reduction. *Environ. Sci. Technol.* **2021**, *55*, 10821−10831.
(62) Bai, Y.; Subdiaga, E.; Haderlein, S. B.; Knicker, H.; Kappler, A. High-pH and anoxic conditions during soil organic matter extraction increases its electron-exchange capacity and ability to stimulate microbial Fe(III) reduction by electron shuttling. *Biogeosciences* **2020**, *17*, 683−698.
(63) Pi, K.; Markelova, E.; Zhang, P.; Van Cappellen, P. Arsenic oxidation by flavin-derived reactive species under oxic and anoxic conditions: oxidant formation and pH dependence. *Environ. Sci. Technol.* **2019**, *53*, 10897−10905.
(64) Katsoyiannis, I. A.; Ruettimann, T. R.; Hug, S. J. pH dependence of Fenton reagent generation and As(III) oxidation and removal by corrosion of zero valent iron in aerated water. *Environ. Sci. Technol.* **2008**, *42*, 7424−7430.
(65) Buxton, G. V.; Greenstock, C. L.; Helman, W. P.; Ross, A. Critical review of rate constants for reactions of hydrated electrons, hydrogen atoms and hydroxyl radicals (•OH/•O^- in aqueous solution. *J. Phys. Chem. Ref. Data* **1988**, *17*, 513−886.
(66) Xu, T.; Zhu, R.; Shang, H.; Xia, Y.; Liu, X.; Zhang, L. Photochemical behavior of ferrihydrite-oxalate system: Interfacial reaction mechanism and charge transfer process. *Water Res.* **2019**, *159*, 10−19.
(67) Bielski, B. H. J.; Cabelli, D. E.; Arudi, R. L.; Ross, A. B. Reactivity of HO_2/O_2^- radicals in aqueous solution. *J. Phys. Chem. Ref. Data* **1985**, *14*, 1041−1100.
(68) Liu, W.; Andrews, S. A.; Stefan, M. I.; Bolton, J. R. Optimal methods for quenching H_2O_2 residuals prior to UFC testing. *Water Res.* **2003**, *37*, 3697−3703.
(69) Gómez-Toribio, V.; Martínez, A. T.; Martínez, M. J.; Guillén, F. Oxidation of hydroquinones by the versatile ligninolytic peroxidase from *Pleurotus eryngii*. *Eur. J. Biochem.* **2001**, *268*, 4787−4793.
(70) Thurman, E. M.; Malcolm, R. L. Preparative isolation of aquatic humic substances. *Environ. Sci. Technol.* **1981**, *15*, 463−466.
(71) Lv, J.; Miao, Y.; Huang, Z.; Han, R.; Zhang, S. Facet-mediated adsorption and molecular fractionation of humic substances on hematite surfaces. *Environ. Sci. Technol.* **2018**, *52*, 11660−11669.
(72) Chen, W.; Westerhoff, P.; Leenheer, J. A.; Booksh, K. Fluorescence excitation-emission matrix regional integration to quantify spectra for dissolved organic matter. *Environ. Sci. Technol.* **2003**, *37*, 5701−5710.
(73) Rose, M. T.; Patti, A. F.; Little, K. R.; Brown, A. L.; Jackson, W. R.; Cavagnaro, T. R. A meta-analysis and review of plant-growth response to humic substances. *Adv. Agron.* **2014**, *124*, 37−89.

https://doi.org/10.1021/acs.est.2c03799
Environ. Sci. Technol. XXXX, XXX, XXX−XXX